Macromolecules

Article

pubs.acs.org/Macromolecules

Multiphoton Harvesting in an Angular Carbazole-Containing Zn(II)-Coordinated Random Copolymer Mediated by Twisted Intramolecular Charge Transfer State

Tingchao He,[†] Yang Gao,[‡] Rui Chen,[†] Lin Ma,[†] Deepa Rajwar,[‡] Yue Wang,[†] Andrew C. Grimsdale,*[,‡] and Handong Sun*[,†,§]

[†]Division of Physics and Applied Physics, School of Physical and Mathematical Sciences, Nanyang Technological University, 21 Nanyang Link, Singapore 637371, Singapore

[‡]School of Materials Science and Engineering, Nanyang Technological University, Singapore 639798, Singapore

[§]Centre for Disruptive Photonic Technologies (CDPT), Nanyang Technological University, Singapore 637371, Singapore

Supporting Information

ABSTRACT: Multiphoton excited fluorescent probes with highly emissive, photostable, low cytotoxic properties are very important for photodynamic therapy, sensing, and bioimaging, etc., even though still challenging. Here, we report the synthesis and spectroscopic studies of two statistical Zn(II)-coordinated copolymers containing different donor types and the same acceptor type (a dithienylbenzothiadiazole-based ditopic terpyridine ligand), aiming to achieving efficient multiphoton harvesting systems. Our results indicate that an angular carbazole-based ditopic terpyridine ligand donor shows a strong tendency to form a twisted intramolecular charge transfer (TICT) state. Taking advantage of the large multiphoton absorption coefficient in the donor and efficient Förster resonance energy transfer (FRET) mediated by TICT state, efficiently enhanced fluorescence from the acceptor under two- and even three-photon excitation is consequently achieved. In contrast, for a linear carbazole-based ditopic terpyridine ligand donor, the enhanced multiphoton excited fluorescence from the acceptor originates from reabsorption effect instead of FRET. For the first time, we have reported the multiphoton harvesting properties of metal−organic complexes, especially stressing the crucial role of TICT state in multiphoton excited FRET, which sheds light on how to design efficient multiphoton harvesting systems in general.

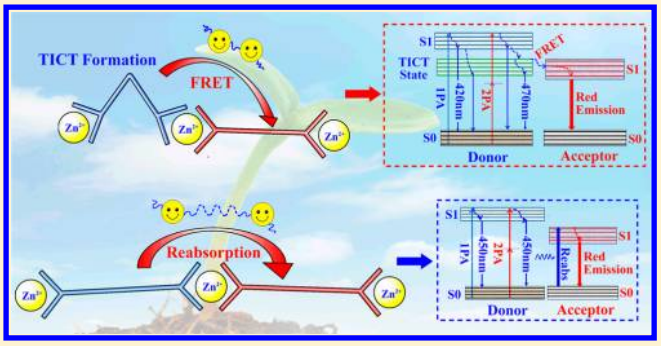

1. INTRODUCTION

Compared to small organic molecules, conjugated polymers usually exhibit large multiphoton absorption (MPA) due to their large number of repeat units and thus possess great potential applications in biological imaging and nonlinear optical devices.[1] However, the MPA cross sections per repeat unit of conjugated polymers are still relatively low (typically from tens to several hundred GM for two-photon absorption, abbreviated as TPA, 1 GM = 1×10^{-50} cm^4 s molecules^{-1} photon^{-1}), which leaves much room for further improvement. Regarding the strategies for molecular design, utilizing Förster resonance energy transfer (FRET) within multichromophores has been proved to be a good approach to achieving efficient multiphoton absorbing materials.[2] A number of methods have been developed to design to optimize multiphoton artificial light harvesting systems, including both covalent and non-convalent methods for linking the component chromophores.[3] However, the covalent method has the disadvantage of low synthetic efficiency though it can produce arrays with large numbers of chromophores. Noncovalent methods, such as self-assembly, might overcome this problem.

Among the various self-assembled supramolecules made for possible application in light-harvesting systems, metal−ligand complex (MLC) based energy transfer systems have received much attention, due to their crystalline nature, and the well-determined distances and angles between the units.[4] These materials thus combine the beneficial properties of both metal ion complexes and polymer backbones. By varying the metal−ligand combination, the binding strength, reversibility, and solubility of the MLCs and thus their optoelectronic properties can be readily tuned. It is noteworthy that Hupp et al. reported long-range energy migration in a metal−organic framework (MOF) with an exciton migration distance up to 45 porphyrin struts.[5] They also showed that a pillared-paddlewheel type MOF featuring bodipy- and porphyrin-based struts was capable of harvesting light spanning the entire visible spectrum.[6] Lin et al. clearly demonstrated the facile intracrystalline site-to-site energy migration dynamics in Ru(II)/Os(II) (2,2′-bipyridine)$_3$-

Received: December 23, 2013
Revised: January 29, 2014
Published: February 7, 2014

Scheme 1. Chemical Structures of Ligands 1, 2, and 3, Homo-oligomers Zn-1, Zn-2, and Zn-3 (Acceptor), and Copolymers P1 and P2

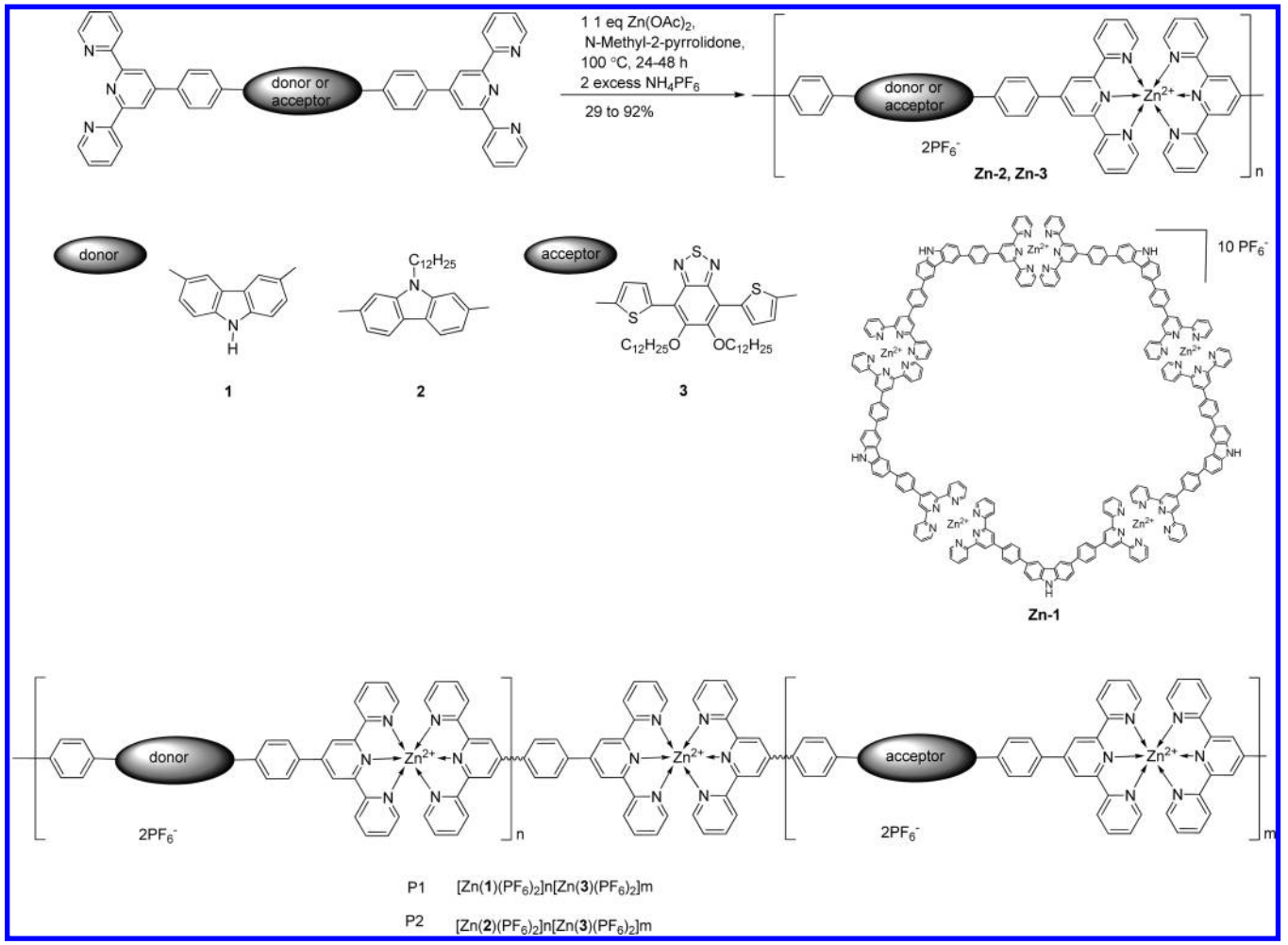

derived MOFs through luminescence quenching measurements.[7] Moreover, it was demonstrated that MOFs can be further functionalized using colloidal quantum dots (QDs) for the enhancement of light harvesting via energy transfer from the QDs to the MOFs.[8] However, there are very few studies that reveal under what circumstances FRET systems can be obtained with MLCs. More strikingly, there has been no report about the multiphoton excited FRET in MLCs, even though such vision may hold broad prospects for applications in biological imaging and nonlinear optical devices.

In various MLCs, the coordination of transition metal ions such as Zn(II) ions with terpyridines has been proved to be a productive way for the synthesis of optoelectronic materials due to the high binding affinity of terpyridines toward transition metal ions in low oxidation states.[9] On the one hand, Zn(II) ions represent considerable advantages over other potential metals because of their abundance and low cost. On the other hand, well-defined structures and enhanced optical properties can be achieved in Zn(II)-coordinated metallopolymers because the full d electrons in Zn(II) do not quench the fluorescence from the conjugated ligands. More interestingly, statistical polymers from cocoordination of different types of ligands in desired stoichiometric ratios will allow the manipulation of energy transfer processes.[4b,c] Inspired by the few previous reports of energy transfer under one-photon excitation in such materials, we decided to explore them using multiphoton excitation, with the aim of broadening their related applications, such as bioimaging, optical limiting, upconverted lasing, etc.[1b] In this work, two types of angular and linear carbazole based ditopic terpyridine ligands were designed as donors. Subsequently, two Zn(II) terpyridine random copolymers are respectively synthesized by the cocoordination of the related donor and acceptor (dithienylbenzothiadiazole-based ditopic terpyridine ligand). These combinations facilitate efficient energy transfer from the excited donor part to the acceptor moiety, which is studied by using comprehensive spectroscopic analysis. We present the first study on multiphoton excited FRET processes in the metal-coordinated copolymers, which are of importance for the applications in bioimaging and nonlinear optical devices. Moreover, different from previous studies, we focus on the influences of the molecular geometry of the MLCs on the formation of twisted intramolecular charge transfer (TICT) state with long-lived lifetime, which plays the critical role in the resultant efficient FRET.

2. EXPERIMENTAL SECTION

2.1. Synthesis and Materials. Two new bisterpyridine ligands **1** and **2** were synthesized through the Suzuki coupling method,[9c] and the metallopolymerization was carried out according to slightly modified literature procedures,[4c] by heating the ligands and Zn(II) ions with desired molar ratios in *N*-methylpyrrolidone, exchanging counterion of

dx.doi.org/10.1021/ma402623z | *Macromolecules* 2014, 47, 1316−1324

acetate to hexafluorophosphate, and thorough washing with DCM, MeOH, with all structural data attached in the Supporting Information.

The chemical structures of the materials used in this work are shown in Scheme 1. Two different types of carbazole-based ditopic terpyridine ligands **1** and **2** were selected as the donor units, with terpyridine part linked to the 3,6-positions of carbazole in **1** and the 2,7-positions in **2** with an alkyl chain at the 9-position to make it more soluble in organic solvents. In order to evaluate the influence of geometry on the energy transfer process, using zinc ions, by cocoordination of monomers **1** and **2** with dithienylbenzothiadiazole-based ditopic terpyridine (ligand **3**) as the acceptor unit, **P1** and **P2** were designed and synthesized, respectively. Equal moles of the donor ligand and acceptor ligand were chosen for preparation of copolymers to resemble the component ratio of alternating copolymers linked with covalent bonds through cross-coupling, which was vastly used as optical and optoelectronic materials. In view of the dynamic nature of the Zn(II)−terpyridine complexation, statistical copolymers other than truly alternating Zn(II)−terpyridine copolymers were obtained. Usually, instead of the monomers, their metal complexes were used as donors to study the energy transfer process in statistical copolymers. Therefore, Zn(II) complexes of **1** and **2** were also synthesized (Scheme 1). Homocoordination of the those two with zinc ions showed geometry-dependent behaviors, wherein the zinc coordination of ligand **1** afforded a pentamer (**Zn-1**) with well-defined signals with distinct splitting in NMR and characteristic MS signals while zinc coordination of ligand **2** afforded an extended oligomer (**Zn-2**) with broad NMR signals. It could be concluded that, in Zn(II) complexes, the individual monomer unit **1** was arranged within a pentameric ring in homo-oligomer **Zn-1** while the monomer **2** was arranged in a quasi-linear manner in homo-oligomer **Zn-2**. However, in the copolymer **P1**, the individual monomer **1** was indeed aligned in a long chain and was randomly interrupted by the acceptor. Hence, the photophysical data of monomer **1** was considered more suitable than that of **Zn-1** as the reference for studying the copolymer **P1**, while **Zn-2** could be directly considered to be the donor for **P2**. In the following parts, we only discussed the optical properties of **1**, **P1**, **Zn-2**, and **P2** while the detailed spectroscopic information for **2** and **Zn-1** was depicted in the Supporting Information (Figures S2−S5).

2.2. Characterization. Nuclear magnetic resonance (NMR) spectra (^{1}H and ^{13}C) were recorded on a Bruker Advance 400 spectrometer. Mass spectra were recorded using a Shimadzu Axima matrix-assisted laser desorption/ionization time-of-flight (MALDI-TOF) mass spectrometer. UV−vis absorption spectra were measured with a Shimadzu UV−vis spectrophotometer. For the measurements of excitation wavelength-dependent fluorescence spectra under one-photon excitation, femtosecond pulses (100 fs, 1000 Hz) were used as excitation source. The fluorescence spectra of the samples were collected from the solutions filled in cuvettes with a path length of 1 cm. The signals were dispersed by a 750 mm monochromator combined with suitable filters and detected by a photomultiplier tube (Hamamatsu R928) using a standard lock-in amplifier technique. Excitation spectra were obtained using a 450 W xenon lamp monochromated with a double Czerny-Turner spectrometer (GEMINI 180) whose excitation intensity was precorrected.

2.3. Measurements of Two- and Three-Photon Excited Fluorescence Spectra. Multiphoton excited fluorescence spectra were excited by using a Ti:sapphire laser, which produced 100 fs (HW1/e) pulses in the wavelength range of 260−2600 nm and at a repetition of 1000 Hz. In the measurement process, the input laser beam was focused into the samples. The fluorescence was collected at an angle of 90° to the incoming excitation beam, and then the signals were measured with the same method used for one-photon excited fluorescence spectra.

2.4. Measurements of TPA Cross Sections. TPA coefficients of cross sections were determined by using the Z-scan technique.[10] The samples were dissolved and placed in 1 mm quartz cuvettes. The excitation source was the same as that used for the measurements of two-photon excited fluorescence. The detailed data processing method can be found in ref 10.

2.5. Lifetime Measurements and Time-Resolved Fluorescence Spectra. The measurements of lifetime and time-resolved fluorescence spectra were carried out by using an Optronis Optoscope streak camera system, which has an ultimate temporal resolution of ~50 ps. The laser pulses from an OPA combined with TOPAS (1000 Hz, 100 fs, Spectra-Physics, Inc.) with the wavelength of 360 nm were used as excitation source.

3. RESULTS AND DISCUSSION

3.1. Linear Optical Properties of 1 and Zn-2. Under the one-photon excitation of 360 nm (100 fs, 1000 Hz), there were dual emission bands from monomer **1**, peaked at ~420 and ~470 nm, respectively, as shown in Figure 1a. Their relative

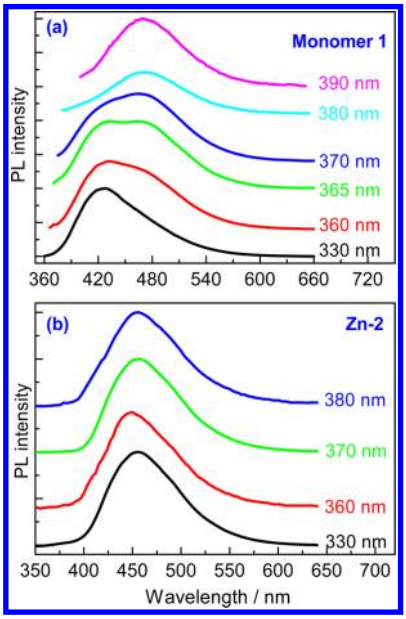

Figure 1. Wavelength-dependent one-photon excited fluorescence spectra for monomer **1** (a) and **Zn-2** (b) in DMSO solutions with a concentration of 1×10^{-5} M.

intensities depended significantly on the excitation wavelengths. When a shorter excitation wavelength (<360 nm) was used, the spectrum was dominated by the emission at 420 nm. The emission at 470 nm monotonically increased and eventually surpassed the emission at 420 nm as the excitation wavelength became longer. For **Zn-2**, only the emission at 454 nm was observed (Figure 1b), regardless of the excitation wavelength.

The wavelength-dependent emission properties of monomer **1** should not be induced by the vibronic levels of excited state, which cannot lead to such significant variations in the emission spectra. Undoubtedly, the dual emission bands in monomer **1** indicated the existence of two close-lying emitting states. There are several possible phenomena resulting in dual emission behavior, such as the formation of excimers,[11] dimers,[12] H/J-aggregates,[13] and TICT.[14] However, the mechanism for dual emission bands should be dominated by TICT, which we demonstrate as follows. As depicted in Figure 2a, the emission spectra profiles over a wide range of concentration (5×10^{-8}−5×10^{-5} M) were measured. At the excitation wavelength of 370 nm (100 fs, 1000 Hz), the intensity ratio of dual emission bands remained unchanged, excluding the possibility that the emission band at 470 nm originated from the formation of an excimer. This was because the emission intensity of an excimer state would depend strongly on the solution concentrations.[15]

dx.doi.org/10.1021/ma402623z | Macromolecules 2014, 47, 1316−1324

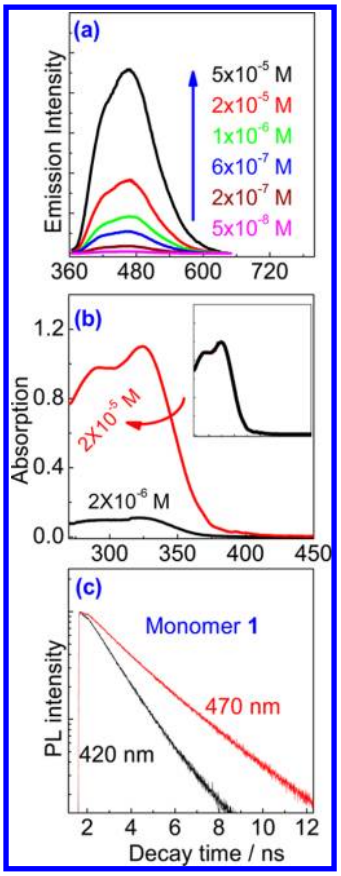

Figure 2. (a) Fluorescence emission spectra of monomer **1** in DMSO solutions as a function of concentration, excited at 370 nm (100 fs, 1000 Hz). (b) UV−vis absorption spectra of monomer **1** with different concentration in DMSO solutions. The inset: normalized absorption spectra of monomer **1** with the respective concentration, indicating that the absorption profile remains unchanged. (c) Fluorescence decay behavior of monomer **1** with a concentration of 1×10^{-5} M in DMSO solution, monitoring the emission at 420 and 470 nm, respectively.

Dimer formation and H/J-aggregates could also be excluded since the formation of a dimer would cause an additional absorption shoulder at longer wavelength,[12] while an H/J-aggregate would result in a noticeable blue/red-shift in absorption spectrum.[13] However, neither an absorption shoulder nor a blue/red-shifted spectrum was observed at higher concentrations (Figure 2b). Moreover, as an excimer site would be populated by intramolecular energy migration, it could only exist simultaneously with the monomer state regardless of the excitation wavelengths used. Therefore, the emission band at 470 nm for monomer **1** was unambiguously assigned to TICT state emission. In polar and/or viscous medium, upon excitation, two stable conformations would be formed by twisting the electron-donating and electron-accepting moieties in monomer **1**, one with respect to the other.[14a] The planar conformation had only a weak charge transfer character to form locally excited (LE) state that emitted fluorescence at 420 nm whereas the twisted conformation had complete charge separation, resulting in the highly stabilized TICT state giving fluorescence at 470 nm.[14a] As is well-known, there are two factors that can influence the formation of TICT.[13a] One is the molecular structure, while the other is external environment, such as solvent and temperature. TICT can appear in an orthogonal conformation because the system is decoupled with a zero overlap of the orbitals involved. The molecules with intrinsically distorted conformation or the substituents that can sterically hinder the coplanar (quinoid) structure will favor the appearance of TICT, while those with fixed rigid structure can only emit LE state emission.[13c] The intrinsically angular structure of monomer **1** would thus facilitate the formation of TICT. On the contrary, the relatively coplanar structure of **Zn-2** greatly restricted the intramolecular rotation and rigidified the molecular conformation, emitting exclusively the LE state fluorescence. As for the influences of solvent, the high hydrophilicity of DMSO would exert different interactions with monomer **1** or **Zn-2**.[13a,c] The amido group in monomer **1** made it more hydrophilic, and its twisted molecular conformation was more easily stabilized by the solvating effect of the polar solvent. As a results, the TICT state emerged in monomer **1**. Regarding the more hydrophobic **Zn-2**, its interaction with DMSO was much weaker, further resulting in the much less twisted molecular conformation and absence of TICT.

We have measured the fluorescence lifetime of the emission bands at 420 and 470 nm, respectively, as depicted in Figure 2c. For the emission at 420 nm, its lifetime (1.35 ns) was much shorter than that at 470 nm (2.5 ns). Meanwhile, it was interesting to note that the TICT state emission at 470 nm for monomer **1** exhibited good photostability, which would provide great advantages in its related applications (Figure S1, Supporting Information). Later, we would demonstrate the crucial role of TICT state in the enhanced multiphoton excited fluorescence through FRET process.

3.2. TPA Properties of 1 and Zn-2. Under two-photon excitation, the fluorescence profiles of monomer **1** plotted in Figure 3a showed wavelength-dependent dual emission bands, which was consistent with the case of one-photon excitation. It can be clearly concluded here that under both one- and two-photon excitation the molecules could access the same electronic states, although the relative contribution of the two states was slightly different in each case. As was expected, the fluorescence spectrum profile of **Zn-2** was independent of

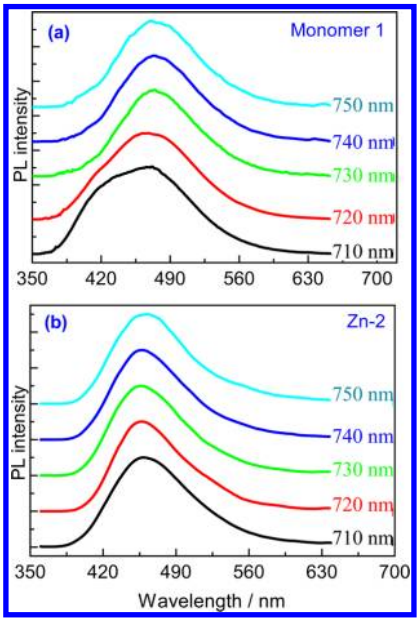

Figure 3. Wavelength-dependent two-photon excited fluorescence spectra of monomer **1** (a) and **Zn-2** (b) in DMSO solutions with a concentration of 2×10^{-5} M.

dx.doi.org/10.1021/ma402623z | Macromolecules 2014, 47, 1316−1324

excitation wavelength under one- and two-photon excitation, as shown in Figure 3b.

Prior to the investigation of TPA properties of copolymers, TPA cross sections of monomer **1** and **Zn-2** in DMSO solutions, at a concentration of 2×10^{-5} M, were measured with the femtosecond Z-scan technique.[10] From the TPA spectra presented in Figure 4, the maximum TPA cross-section

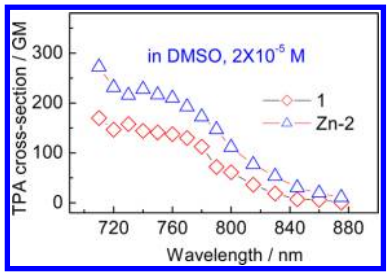

Figure 4. TPA spectra for monomer **1** and **Zn-2** in DMSO solutions. The TPA cross-section values were calculated based on per repeat unit.

values per repeat unit for monomer **1** and **Zn-2** were 170 and 272 GM, respectively. Obviously, **Zn-2** exhibited larger TPA cross section compared to monomer **1**. It was because that the increased conjugation length of **Zn-2** favored intramolecular charge transfer and thus enhanced its TPA cross sections.[16]

In order to well understand the multiphoton excited energy transfer process, we first investigated the one-photon excited energy transfer in copolymers. From the resultant experimental results, we could easily achieve the important information that was indispensable to analyze the corresponding physical mechanisms of energy transfer under multiphoton excitation. This was undoubtedly allowed due to their intrinsically same excitation and emission process.[17]

3.3. One-Photon Excited Energy Transfer in Copolymers P1 and P2. From the linear absorption spectra of **P1** and **P2**, as shown in Figure 5, we could conclude that the electronic coupling between the donor and acceptor in both of them was

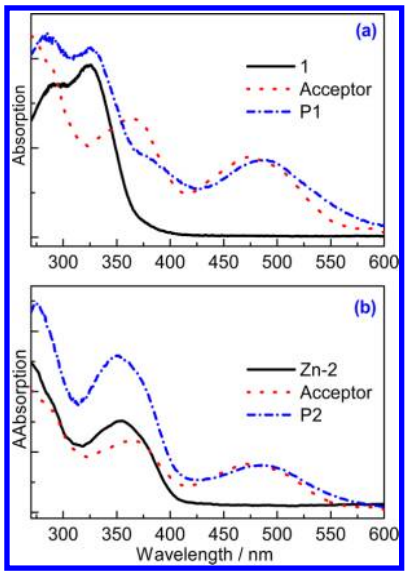

Figure 5. One-photon absorption spectra of monomer **1** (donor **1**), **Zn-2** (donor **2**), acceptor, **P1**, and **P2** in DMSO solutions. The individual absorption characteristics of the donor and acceptor could be observed in the absorption spectra of **P1** and **P2**.

negligibly small. Considering the same acceptor used in **P1** and **P2**, the dramatically different energy transfer processes in the copolymers should be caused by the differences in the donors' excited state confirmations. On the one hand, the long lifetime of TICT state as well as the good spectral overlap between donor emission and acceptor absorption would be beneficial for the occurrence of FRET in **P1**.[18] As for **P2**, the short lifetime of **Zn-2** means FRET competes unfavorably with other deactivation processes which disfavors the FRET process. On the other hand, thanks to the resultant TICT state in monomer **1**, the relative orientation between emission transition dipole of the donor and absorption transition dipole of acceptor is favorable for FRET. On the contrast, in the copolymer **P2**, the dipole orientation between **Zn-2** and acceptor is unfavorable for FRET.[19]

Considering the good overlap between the fluorescence spectra of monomer **1** or **Zn-2** with the absorption spectra of acceptor, as shown in Figure 6a,b, efficient energy transfer may be expected in the random copolymers. Meanwhile, due to their electrostatic interaction in random polymers, donor and acceptor were brought into close proximity to ensure efficient energy transfer between them.[4b,c,20] As was expected, under the excitation of 360 nm (100 fs, 1000 Hz), the fluorescence

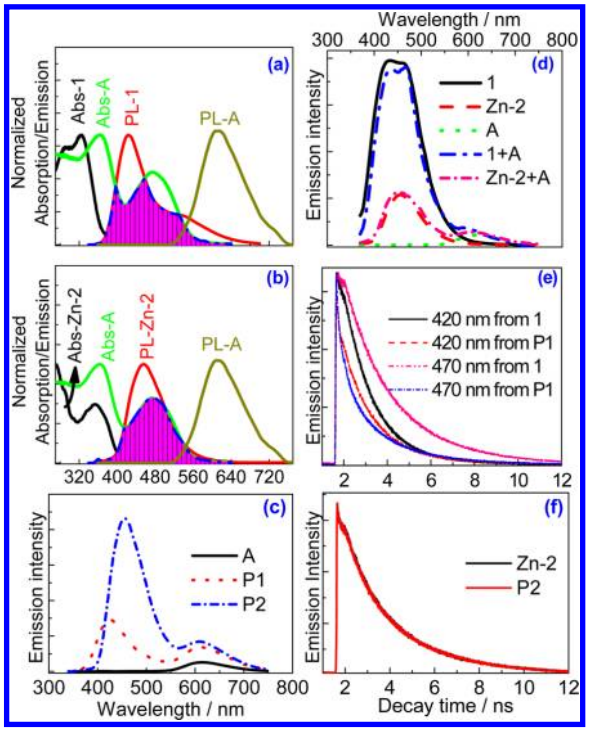

Figure 6. (a, b) Comparison of normalized absorption and fluorescence spectra of donor and acceptor in the copolymers. The spectral overlaps between donor and acceptor in **P1** and **P2** are highlighted in blue. All the measurements are carried out with DMSO solutions. The fluorescence spectra are excited at 360 nm (100 fs, 1000 Hz). (c) Comparison of fluorescence intensity of the copolymers with their corresponding acceptors. They are dissolved into DMSO solutions with a concentration of 1×10^{-5} M and are excited at 360 nm (100 fs, 1000 Hz). (d) Comparison of fluorescence spectra of individual donor and acceptor and their physical blends. (e) Fluorescence decay curves detected at 420 and 470 nm for monomer **1** and **P1** in DMSO solutions, excited at 365 nm. (f) Fluorescence decay curves detected at 450 nm for **Zn-2** and **P2** in DMSO solutions, excited at 365 nm.

dx.doi.org/10.1021/ma402623z | *Macromolecules* 2014, 47, 1316−1324

intensity of **P1** and **P2** (dissolved into DMSO with a concentration of 1×10^{-5} M) increased by about 4 times compared to pure acceptor, as shown in Figure 6c. However, a simple mixture of the involved donor and acceptor revealed no indication of energy transfer (Figure 6d), which was expected because of the large distance between donor and acceptor in the diluted solutions. Therefore, the Zn(II) coordination played a crucial role in the mediation of such an energy transfer in the corresponding Zn(II)-based random copolymer. In order to confirm the energy transfer mechanisms in the copolymers, concentration-dependent or/and time-resolved fluorescence measurements monitoring their corresponding donors emission were carried out. From Figure 6e, the donor fluorescence decay in **P1** was significantly accelerated with respect to that of pure monomer **1**, no matter detected at 420 or 470 nm. It was thus assumed that the shortening of lifetime of donor was dominated by FRET process in **P1**.[21] In contrast, the fluorescence decay of **Zn-2** monitoring at 454 nm, as depicted in Figure 6f, was identical to that measured in **P2**, indicating that reabsorption rather than FRET was responsible for the enhanced emission in **P2**.

In addition, after carefully taking into account the overlap absorption of donor and acceptor, the quantum yield of monomer **1** decreased from 18.5% to 9.6% in **P1**, while the quantum yield of donor in **P2** was almost the same as that of **Zn-2** (15.5%), further confirming the different energy transfer mechanisms in **P1** and **P2**.[22] Meanwhile, it was observed that **P1** exhibited a pronounced quenching (nearly 95%) of the emission at 470 nm while there was large-residue emission at 420 nm, indicating their distinct differences between TICT and LE states during the energy transfer process. Furthermore, the energy transfer efficiencies were calculated to be 59% and 73% for the emission bands at 420 and 470 nm, respectively. Considering there was no FRET process in **P2**, similarly, the LE state of monomer **1** could not directly transfer the absorbed energy to acceptor in a FRET way. The shortening of lifetime at 420 nm should be due to the nonradiative relaxation of energy from LE state to TICT state.

The dynamics of energy transfer process from LE state to TICT state in monomer **1** can be clearly seen from the temporal evolution of fluorescence spectra as shown Figure 7. Within initial about 50 ps after excitation at 360 nm, the fluorescence of monomer **1** was dominated by the emission band at 420 nm while the band at 470 nm was negligible. As time passed, the intensity of emission band at 470 nm increased sharply and eventually resembled the steady state fluorescence spectra in about 120 ps, revealing the ultrafast exciton recycling process (or the migration of excitation energy) from LE state to TICT state. As a result, in **P1**, besides the direct FRET from TICT state to acceptor, the TICT state would capture energy from nearby LE state, resulting in the indirect nonradiative energy transfer from LE state to acceptor.

As sketched in Figure 8, this process was similar to the trap state-mediated FRET in colloidal quantum dots. However, in our case, the intermediate was a TICT state rather than a trap state.[23] Accordingly, the energy transfer rates were calculated to be 1.17×10^9 s^{-1} for the emission band at 470 nm with a Förster distance (R_0), at which the energy transfer efficiency became 50%, of 27 Å (see Supporting Information for detailed calculations). Though the energy transfer rates were relatively smaller compared to some examples,[21a,24] they were comparable to or larger than those of many reported energy transfer systems.[25]

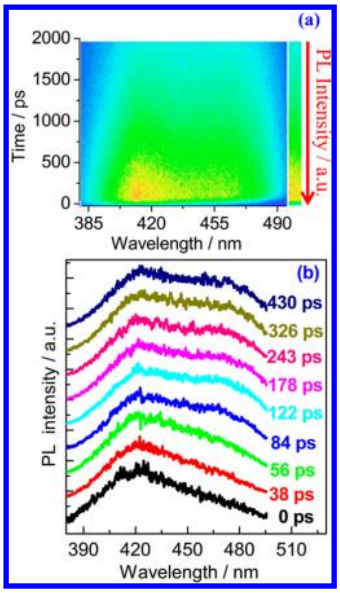

Figure 7. (a) Time-resolved fluorescence image of monomer **1** in DMSO solution with a concentration of 10^{-5} M, excited at 360 nm (100 fs, 1000 Hz). (b) Temporal evolution of fluorescence spectra of monomer **1**.

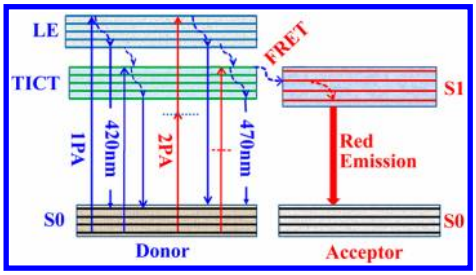

Figure 8. Diagram sketches the energy transfer process in copolymer **P1**. Upon the excitation of one and two photons, besides FRET from the TICT state to acceptor, the energy in the LE state, through nonradiative decay to TICT state, will be recycled and then be transferred to acceptor, which finally attributes to FRET induced fluorescence enhancement of acceptor as well as the reduction of reabsorption effect.

3.4. Two-Photon Excited Energy Transfer in Copolymers P1 and P2. Considering the dramatic enhancement of one-photon excited fluorescence in **P1** and **P2** and strong TPA properties of donors, the studies on two-photon excited fluorescence properties of the copolymers were further carried out. It was found that the donor emission was completely quenched in **P1** and **P2**, accompanied by the simultaneous enhancement of acceptor's two-photon excited fluorescence (Figure S6, Supporting Information). As was expected, over a wide excitation range from 700 to 920 nm, compared to acceptor, two-photon excited fluorescence of **P1** and **P2** was also conspicuously amplified, as depicted in Figure 9a. Consequently, two-photon excited fluorescence of both **P1** and **P2** gave a maximum enhancement factor of 3. Considering the different enhancement factors under one- and two-photon excitation, some explanations were given here. On the one hand, TPA cross sections of donor and acceptor were different from those under one-photon excitation. One the other hand, under one-photon absorption, partial emission from a LE state would be reabsorbed directly by the acceptor, which would also contribute to one-photon excited fluorescence enhancement of

dx.doi.org/10.1021/ma402623z | Macromolecules 2014, 47, 1316−1324

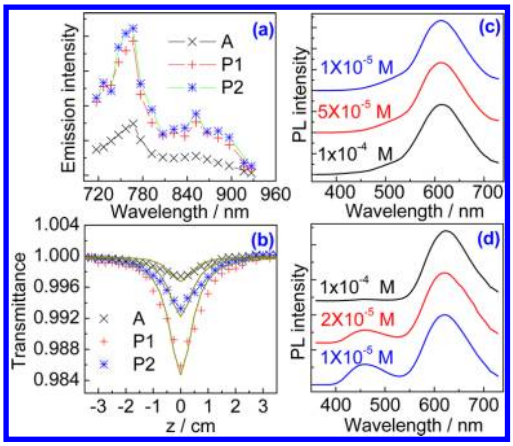

Figure 9. (a) Two-photon excited fluorescence intensity of **P1**, **P2**, and acceptor in DMSO solutions with a concentration of 1×10^{-4} M under different excitation wavelengths. (b) Open Z-scan curves of acceptor, **P1** and **P2** in DMSO solutions with a concentration of 1×10^{-4} M, excited at 760 nm with an excitation intensity of 39 GW/cm^2. Concentration dependent two-photon excited fluorescence spectra of **P1** (c) and **P2** (d), excited at 730 nm.

acceptor. However, the two-photon excited fluorescence emission of donor was dominated by the TICT state emission at 470 nm (Figure 3a), the two-photon excited FRET process should mainly proceed via the TICT state, with a little contribution from reabsorption effect. The TPA cross sections of copolymers were determined using open Z-scan measurements (Figure 9b). As an example, at the excitation wavelength of 760 nm, the values of TPA cross section for **P1** and **P2** were calculated as 2475 and 1160 GM per repeat unit, which were 5.0 and 2.3 times larger than that of acceptor. The resultant values for the entire polymer chain were thus extremely large, favoring their practical applications. Moreover, in order to further confirm the different enhancement mechanisms for **P1** and **P2**, the concentration dependence of two-photon excited fluorescence spectra of copolymers were also measured, as depicted in Figure 9c,d. Apparently, the two-photon excited fluorescence profile for **P1** remained constant over the concentration range from 1×10^{-5}–5×10^{-4} M, which is consistent with the concentration-independent nature of FRET. The observed energy transfer process in **P1** could be briefly discussed as follows. The LE state and TICT state were first populated through two-photon excitation. Instead of emitting fluorescence from them to ground state, the donor transferred the absorbed energy to acceptor by FRET, leading to the large two-photon excited fluorescence enhancement of **P1**.[26] Similar to the case of one-photon excitation, the two-photon excited FRET process in **P1** was also sketched in Figure 8. In contrast, the emission spectra of **P2** suffered from dramatic changes at different concentrations. Specifically, the donor emission in **P2** significantly decreased as the concentration increased, clearly indicating the occurrence of concentration related reabsorption, which was consistent with the lifetime measurement results.

3.5. Three-Photon Excited Energy Transfer in Copolymers P1 and P2. For the materials with visible fluorescence, the excitation wavelengths for three-photon excitation usually fall into the second near-infrared (NIR) region (1000–1400 nm), which has exhibited great advantages in *in vivo* fluorescence imaging, in comparison to the first NIR window used for two-photon excitation (650–950 nm), due to reduced scattering by tissues, deeper tissue penetration, improved resolution, higher sensitivity, and decreased photodamage and photobleaching.[27] However, the major factor that limits its application is that the most fluorescence probes have very small three-photon absorption (3PA) cross sections and dim fluorescence signals. Similar to the case of two-photon excited energy transfer process, three-photon excited energy transfer process can also be expected if the donors have large 3PA. Such a process can also be used to amplify the three-photon excited fluorescence of acceptor. It was also noteworthy that both monomer **1** and **Zn-2** could give rise to strong fluorescence under the excitation 1100 nm, as shown in Figure 10a. The

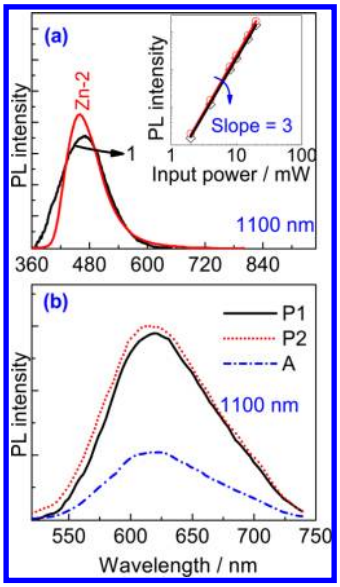

Figure 10. (a) Three-photon excited fluorescence spectra for monomer **1** and **Zn-2** in DMSO solutions with a concentration of 2×10^{-5} M at the wavelength of 1100 nm with optical intensity of 100 GW/cm^2. The inset: cubic dependence of emission intensity on the excitation intensity at 1100 nm, for both monomer **1** and **Zn-2**, confirming the process of 3PA. (b) Comparison of three-photon excited fluorescence spectra of **P1**, **P2**, and acceptor in DMSO solutions with a concentration of 1×10^{-4} M at 1100 nm.

linear dependence of fluorescence intensity on the cubic of the excitation intensity, as shown in the inset of Figure 10a, confirms that 3PA is the main mechanism of their strong fluorescence.[28] As monomer **1** and **Zn-2** exhibited strong three-photon excited fluorescence, fluorescence enhancement may be also achieved in **P1** and **P2** through three-photon excited energy transfer. Actually, at the excitation wavelength of 1100 nm, the emission bands of monomer **1** and **Zn-2** were completely quenched, accompanied by the significant fluorescence enhancement in **P1** and **P2** (Figure 10b). Similar to the discussions above, the fluorescence enhancement of **P1** and **P2** should be induced by three-photon excited FRET or reabsorption effect, respectively.

4. CONCLUSION

For the first time, we herein have demonstrated multiphoton harvesting in Zn(II)-coordinated random copolymers. Rationally designed donors and acceptor have been used in the present study, in order to elucidate the influences of donor structure on energy transfer process. A thorough photophysical study has shown that employing angular carbazole-containing terpyridine ligand as donor is beneficial to enhance multi-

photon excited fluorescence in random copolymers, due to the TICT state mediated FRET process. In contrast, the use of linear carbazole-containing terpyridine ligand as donor does not favor the occurrence of FRET even if there is considerable spectral overlap between donor emission and acceptor absorption. The different energy transfer mechanisms result from the differences in excited-state confirmations between monomer **1** and **Zn-2**. The ability to enhance multiphoton excited red fluorescence in the random copolymer, by the appropriate arrangement of donor structures, presents an exciting opportunity for the construction and optimization of new types of functional photonic applications. Specifically, the revealed crucial role of TICT state shed light on designing novel FRET light harvesting systems. More importantly, due to the properties of low biological toxicity and being environmentally friendly, our nontoxic metal-free multiphoton excited fluorescent polymers may find various applications and are safer than many kinds of semiconductor nanocrystals. Future work will focus on the applications of the polymers, especially for the fabrication of low-cost organic/polymeric biosensing, bioimaging, and optoelectronics materials.

■ ASSOCIATED CONTENT

Supporting Information

Detailed synthetic procedures of ligands **1** and **2**, homo-oligomers **Zn-1** and **Zn-2**, copolymers **P1** and **P2**, molecular weight parameters by ^{1}H NMR, photostability tests and photophysical properties for monomer **1** and **Zn-1**, linear and nonlinear optical properties of monomers **1** and **2**, detailed calculations of energy transfer efficiency parameters, two-photon excited fluorescence spectra of polymers **P1** and **P2**. This material is available free of charge via the Internet at http://pubs.acs.org.

■ AUTHOR INFORMATION

Corresponding Authors

*E-mail: acgrimsdale@ntu.edu.sg (A.C.G.).
*E-mail: hdsun@ntu.edu.sg (H.S.).

Author Contributions

T.H. and Y.G. contributed equally to this work.

Notes

The authors declare no competing financial interest.

■ ACKNOWLEDGMENTS

Financial support from the Singapore Ministry of Education through the Academic Research Fund (Tier 1) through Project No. RG63/10 and from the Singapore National Research Foundation Competitive Research Programs (CRP) under Projects Nos. NRF-CRP5-2009-04 and NRF-CRP6-2010-02 is gratefully acknowledged.

■ REFERENCES

(1) (a) Fang, H.; Lu, S.; Zhan, X.; Feng, J.; Chen, Q.; Wang, H.; Liu, X.; Sun, H. B. *Org. Electron.* **2013**, *14*, 762. (b) Fang, H.; Yang, J.; Ding, R.; Chen, Q.; Wang, L.; Xia, H.; Feng, J.; Ma, Y.; Sun, H. B. *Appl. Phys. Lett.* **2010**, *97*, 101101. (c) He, G. S.; Tan, L.; Zheng, Q.; Prasad, P. N. *Chem. Rev.* **2008**, *108*, 1245. (d) He, T.; Wei, W.; Ma, L.; Chen, R.; Wu, S.; Zhang, H.; Yang, Y.; Ma, J.; Huang, L.; Gurzadyan, G. G.; Sun, H. *Small* **2012**, *8*, 2163. (e) He, T.; Lim, Z. B.; Ma, L.; Li, H.; Rajwar, D.; Ying, Y.; Di, Z.; Girmsdale, A. C.; Sun, H. *Chem.—Asian J.* **2013**, *8*, 564. (f) He, T.; Too, P. C.; Chen, R.; Chiba, S.; Sun, H. *Chem.—Asian J.* **2012**, *7*, 2090. (g) Wang, Y.; Yang, X.; He, T.; Gao, Y.; Demir, H. V.; Sun, X. W.; Sun, H. *Appl. Phys. Lett.* **2013**, *102*, 021917.

(2) (a) Dichtel, W. R.; Serin, J. M.; Edder, C.; J. Fréchet, J. M.; Matuszewski, M.; Tan, L.; Ohulchanskyy, T. Y.; Prasad, P. N. *J. Am. Chem. Soc.* **2004**, *126*, 5380. (b) Oar, M. A.; Serin, J. M.; Dichtel, W. R.; Fréchet, J. M. J. *Chem. Mater.* **2005**, *17*, 2267. (c) Oar, M. A.; Dichtel, W. R.; Serin, J. M.; Fréchet, J. M. J.; Rogers, J. E.; Slagle, J. E.; Fleitz, P. A.; Tan, L.; Ohulchanskyy, T. Y.; Prasad, P. N. *Chem. Mater.* **2006**, *18*, 3682.

(3) (a) Rao, K. V.; Datta, K. K. R.; Eswaramoorthy, M.; George, S. J. *Angew. Chem., Int. Ed.* **2011**, *50*, 1179. (b) He, T.; Qi, X.; Chen, R.; Wei, J.; Zhang, H.; Sun, H. *ChemPlusChem* **2012**, *77*, 688. (c) Sapsford, K. E.; Berti, L.; Medintz, I. L. *Angew. Chem., Int. Ed.* **2006**, *45*, 4562. (d) Halivni, S.; Sitt, A.; Hadar, I.; Banin, U. *ACS Nano* **2012**, *6*, 2758.

(4) (a) D'Souza, F.; Amin, A. N.; El-Khouly, M. E.; Subbaiyan, N. K.; Zandler, M. E.; Fukuzumi, S. *J. Am. Chem. Soc.* **2012**, *134*, 654. (b) Larsen, J.; Puntoriero, F.; Pascher, T.; McClenaghan, N.; Campagna, S.; Åkesson, E.; Sundström, V. *ChemPhysChem* **2007**, *8*, 2643. (c) Schlütter, F.; Wild, A.; Winter, A.; Hager, M. D.; Baumgaertel, A.; Friebe, C.; Schubert, U. S. *Macromolecules* **2010**, *43*, 2759. (d) Happ, B.; Schäfer, J.; Menzel, R.; Hager, M. D.; Winter, A.; Popp, J.; Beckert, R.; Dietzek, B.; Schubert, U. S. *Macromolecules* **2011**, *44*, 6277.

(5) Son, H.; Jin, S.; Patwardhan, S.; Wezenberg, S. J.; Jeong, N. C.; So, M.; Wilmer, C. E.; Sarjeant, A. A.; Schatz, G. C.; Snurr, R. Q.; Farha, O. K.; Wiederrecht, G. P.; Hupp, J. T. *J. Am. Chem. Soc.* **2013**, *135*, 862.

(6) Lee, C. Y.; Farha, O. K.; Hong, B. J.; Sarjeant, A. A.; Nguyen, S. T.; Hupp, J. T. *J. Am. Chem. Soc.* **2011**, *133*, 15858.

(7) Kent, C. A.; Mehl, B. P.; Ma, L.; Papanikolas, J. M.; Meyer, T. J.; Lin, W. *J. Am. Chem. Soc.* **2010**, *132*, 16767.

(8) Jin, S.; Son, H.; Farha, O.; Wiederrecht, G. P.; Hupp, J. T. *J. Am. Chem. Soc.* **2013**, *135*, 955.

(9) (a) Wild, A.; Winter, A.; Schlüttera, F.; Schubert, U. S. *Chem. Soc. Rev.* **2011**, *40*, 1459. (b) He, T.; Rajwar, D.; Ma, L.; Wang, Y.; Lim, Z. B.; Grimsdale, A. C.; Sun, H. *Appl. Phys. Lett.* **2012**, *101*, 213302. (c) Lim, Z. B.; Li, H.; Sun, S.; Lek, J. Y.; Trewin, A.; Lam, Y. M.; Grimsdale, A. C. *J. Mater. Chem.* **2012**, *22*, 6218.

(10) (a) Sheik-Bahae, M.; Said, A. A.; Van Stryland, E. W. *Opt. Lett.* **1989**, *14*, 955. (b) Sheik-Bahae, M.; Said, A. A.; Wei, T. H.; Haga, D. J.; Stryland, E. W. Van. *IEEE J. Quantum Electron.* **1990**, *26*, 760.

(11) Bartholomew, G. P.; Rumi, M.; Pond, S. J. K.; Perry, J. W.; Tretiak, S.; Bazan, G. C. *J. Am. Chem. Soc.* **2004**, *126*, 11529.

(12) (a) Clark, J.; Silva, C.; Friend, R. H.; Spano, F. C. *Phys. Rev. Lett.* **2007**, *98*, 206406. (b) Chaudhuri, D.; Li, D.; Che, Y.; Shafran, E.; Gerton, J. M.; Zang, L.; Lupton, J. M. *Nano Lett.* **2011**, *11*, 488. (c) Würthner, F.; Kaiser, T. E.; Saha-Möller, C. R. *Angew. Chem., Int. Ed.* **2011**, *50*, 3376.

(13) (a) Grabowski, Z. R.; Rotkiewicz, K.; Rettig, W. *Chem. Rev.* **2003**, *103*, 3899. (b) Jin, X.; Ren, C.; Sun, J.; Zhou, X.; Cai, L.; Zhang, J. *Chem. Commun.* **2012**, *48*, 10422. (c) Hu, R.; Lager, E.; Aguilar-Aguilar, A.; Liu, J.; Lam, J. W. Y.; Sung, H. H. Y.; Williams, I. D.; Zhong, Y.; Wong, K. S.; Peña-Cabrera, E.; Tang, B. Z. *J. Phys. Chem. C* **2009**, *113*, 15845.

(14) (a) Revill, J. A.T.; Brown, R. G. *Chem. Phys. Lett.* **1992**, *188*, 433. (b) Shigeta, M.; Morita, M.; Konishi, G. *Molecules* **2012**, *17*, 4452.

(15) (a) Wang, X.; Wang, D.; Zhou, G.; Yu, W.; Zhou, Y.; Fang, Q.; Jiang, M. *J. Mater. Chem.* **2001**, *11*, 1600. (b) Albota, M.; Beljonne, D.; Brédas, J. L.; Ehrlich, J. E.; Fu, J. Y.; Heikal, A. A.; Hess, S. E.; Kogej, T.; Levin, M. D.; Marder, S. R.; McCord-Maughon, D.; Perry, J. W.; Röckel, H.; Rumi, M.; Subramaniam, G.; Webb, W. W.; Wu, X. L.; Xu, C. *Science* **1998**, *281*, 1653.

(16) (a) Yoo, H.; Yang, J.; Yousef, A.; Wasielewski, M. R.; Kim, D. *J. Am. Chem. Soc.* **2010**, *132*, 3939. (b) Sherwood, G. A.; Cheng, R.; Chacon-Madrid, K.; Smith, T. M.; Peteanu, L. A. *J. Phys. Chem. C* **2010**, *114*, 12078. (c) Halkyard, C. E.; Rampey, M. E.; Kloppenburg, L.; Studer-Martinez, S. L.; Bunz, U. H. F. *Macromolecules* **1998**, *31*, 8655. (d) Jancy, B.; Asha, S. K. *Chem. Mater.* **2008**, *20*, 169.

(17) He, F.; Ren, X.; Shen, X.; Xu, Q. *Macromolecules* **2011**, *44*, 373.

(18) (a) Clapp, A. R.; Medintz, I. L.; Fisher, B. R.; Anderson, G. P.; Mattoussi, H. J. *Am. Chem. Soc.* **2005**, *127*, 1242. (b) He, T.; Chen, R.; Lim, Z. B.; Rajwar, D.; Ma, L.; Wang, Y.; Gao, Y.; Grimsdale, A. C.; Sun, H. *Adv. Opt. Mater.* **2014**, *2*, 39.
(19) Ogi, S.; Sugiyasu, K.; Takeuchi, M. *ACS Macro Lett.* **2012**, *1*, 1199.
(20) (a) Bai, F.; Chang, C. H.; Webber, S. E. *Macromolecules* **1986**, *19*, 2484. (b) Qi, X.; Pu, K.; Fang, C.; Wen, G.; Zhang, H.; Boey, F. Y. C.; Fan, Q.; Wang, L.; Huang, W. *Macromol. Chem. Phys.* **2007**, *208*, 2007.
(21) (a) Clapp, A. R.; Medintz, I. L.; Mauro, J. M.; Fisher, B. R.; Bawendi, M. G.; Mattoussi, H. *J. Am. Chem. Soc.* **2004**, *126*, 301. (b) Sun, Y.; Wallrabe, H.; Seo, S.; Periasamy, A. *ChemPhysChem* **2011**, *12*, 46. (c) Förster, T. *Ann. Phys.* **1948**, *2*, 55. (d) Förster, T. In *Fluorezenz Organischer Verbindungen*; Vandenhock & Ruprech: Göttingen, Germany, 1951. (e) Förster, T. *Discuss. Faraday Soc.* **1959**, *27*, 7. (e) Chen, R.; Ta, V. D.; Xiao, F.; Zhang, Q.; Sun, H. D. *Small* **2013**, *9*, 1052.
(22) (a) Didenko, V. V. *Biotechniques* **2001**, *31*, 1106. (b) Rogach, A. L. *Nano Today* **2011**, *6*, 355.
(23) (a) Franzl, T.; Shavel, A.; Rogach, A. L.; Gaponik, N.; Klar, T. A.; Eychmüller, A.; Feldmann, J. *Small* **2005**, *1*, 392. (b) Franzl, T.; Klar, T. A.; Schietinger, S.; Rogach, A. L.; Feldmann, J. *Nano Lett.* **2004**, *4*, 1599. (c) Klar, T. A.; Franzl, T.; Rogach, A. L.; Feldmann, J. *Adv. Mater.* **2005**, *17*, 769. (d) Franzl, T.; Koktysh, D. S.; Klar, T. A.; Rogach, A. L.; Feldmann, J.; Gaponik, N. *Appl. Phys. Lett.* **2004**, *84*, 2904.
(24) Babu, S. S.; Hollamby, M. J.; Aimi, J.; Ozawa, H.; Saeki, A.; Seki, S.; Kobayashi, K.; Hagiwara, K.; Yoshizawa, M.; Möhwald, H.; Nakanishi, T. *Nat. Commun.* **2013**, *4*, 1969.
(25) (a) Cucinotta, F.; Carniato, F.; Devaux, A.; Cola, L. D.; Marchese, L. *Chem.—Eur. J.* **2012**, *18*, 15310. (b) Ramachandra, S.; Popovic, Z. D.; Schuermann, K. C.; Cucinotta, F.; Calzaferri, G.; Cola, L. D. *Small* **2011**, *7*, 1488.
(26) (a) Fan, H.; Guo, L.; Li, K. F.; Wong, M. S.; Cheah, K. W. *J. Am. Chem. Soc.* **2012**, *134*, 7297. (b) Guo, L.; Li, K. F.; Wong, M. S.; Cheah, K. W. *Chem. Commun.* **2013**, *49*, 3597. (c) Brousmiche, D. W.; Serin, J. M.; J. Fréchet, J. M.; He, G. S.; Lin, T.; Chung, S. J.; Prasad, P. N. *J. Am. Chem. Soc.* **2003**, *125*, 1448. (d) He, G. S.; Lin, T.; Cui, Y.; Prasad, P. N.; Brousmiche, D. W.; Serin, J. M.; Fréchet, J. M. J. *Opt. Lett.* **2003**, *28*, 768 (c).
(27) (a) He, G. S.; Bhawalkar, J. D.; Prasad, P. N.; Reinhardt, B. A. *Opt. Lett.* **1995**, *20*, 1524. (b) Bhawalkar, J. D.; He, G. S.; Prasad, P. N. *Rep. Prog. Phys.* **1996**, *59*, 1041.
(28) Yu, J. H.; Kwon, S.; Petrášek, Z.; Park, O. K.; Jun, S.; Shin, K.; Choi, M.; Park, Y.; Park, K.; Na, H. B.; Lee, N.; Lee, D.; Kim, J. H.; Schwille, P.; Hyeon, T. *Nat. Mater.* **2013**, *12*, 359.